MAR 13 1953

RESEARCH MEMORANDUM

COMPARISON OF MEASURED AND PREDICTED INDICATED ANGLES

OF ATTACK NEAR THE FUSELAGES OF A TRIANGULAR-WING

WIND-TUNNEL MODEL AND A SWEPT-WING

FIGHTER AIRPLANE IN FLIGHT

By Norman M. McFadden, John L. McCloud, III,
and Harry A. James

Ames Aeronautical Laboratory
Moffett Field, Calif.

NATIONAL ADVISORY COMMITTEE
FOR AERONAUTICS
WASHINGTON
March 11, 1953

NATIONAL ADVISORY COMMITTEE FOR AERONAUTICS

RESEARCH MEMORANDUM

COMPARISON OF MEASURED AND PREDICTED INDICATED ANGLES

OF ATTACK NEAR THE FUSELAGES OF A TRIANGULAR-WING

WIND-TUNNEL MODEL AND A SWEPT-WING

FIGHTER AIRPLANE IN FLIGHT

By Norman M. McFadden, John L. McCloud, III,
and Harry A. James

SUMMARY

Measurements of the local flow angles near the fuselages of a triangular-wing wind-tunnel model and of an F-86A-5 airplane in flight have been made by the use of air-flow detectors on the fuselages. Comparison of these measured flow angles are made herein with predicted flow angles. The methods used accurately estimated the change in upwash due to flap deflection on the triangular-wing model. However, the potential flow equations used to estimate the upwash due to the presence of the fuselage consistently overestimated the effects of the fuselage at the location of the detectors, which were very near the fuselage but outside the boundary layer. At the detector location on the wind-tunnel model (1.2 semispans forward of the quarter-chord line) the change in upwash due to flap deflection was small and could be neglected for most applications.

INTRODUCTION

Many cruise- and fire-control systems for aircraft and guidance systems for missiles contain computers requiring signals proportional to the true angle of attack. Reference 1 has shown that one feasible method of obtaining the true angle of attack is by the use of detectors which measured the local flow angle (i.e., the indicated angle of attack) near the nose of the fuselage. It was found that for the test airplane the true angle of attack was a linear function of the local flow angle.

There are two questions regarding this method of obtaining the required angle-of-attack signals. One question concerns the possibility of estimating the local flow angle accurately enough to make flight calibration unnecessary, or, at least, accurately enough to enable the choice of the location of the detector to be made with confidence in the airplane design stage and, furthermore, to enable the design of the required computers to be made without waiting for the flight calibrations of the angle-of-attack system. The second question concerns its use on triangular-wing aircraft where elevon deflection might possibly influence the flow at the detector location to such an extent that the calibration and computers required to reduce the local flow angles to true angles of attack would have to use signals proportional to flap deflection as well as angle of attack.

This report presents the results of low-speed wind-tunnel measurements of local flow angles using a detector mounted on the forward portion of the fuselage of a triangular-wing-fuselage model. These test results and test results of reference 1 are compared with values of indicated angle of attack predicted by the methods of reference 2.

NOTATION

$\bar{c}$ mean aerodynamic chord

C_L lift coefficient, $\text{lift} \big/ \left(\frac{1}{2}\rho V^2\right) S$

S wing area, sq ft

V velocity, ft/sec

α angle of attack, deg

δ_f flap deflection, deg

ϵ upwash angle, deg

ρ density, slugs/cu ft

Subscripts

b body

G geometric, referenced to tunnel center line

I   indicated

T   true

w   wing

APPARATUS AND TESTS

An aspect ratio 2 triangular-wing-fuselage model was tested in the Ames 40- by 80-foot wind tunnel with a Specialties, Inc., Type J, Airstream Direction Detector, used to indicate the local flow angle, mounted on the fuselage 1.2 semispans forward of the wing quarter-chord line. Dimensions of the model are given in figure 1.

The Airstream Direction Detector is a pressure actuated null seeking device. The detector has a small cylindrical probe with two lengthwise slots spaced 60° apart which provide differential pressure to rotate the probe to seek the null or zero differential position which is recorded by a potentiometer.

The local flow angles were measured at a tunnel dynamic pressure of 30 pounds per square foot over an angle-of-attack range of 0° to 8° and with a flap deflection range of ±15°. Since the detector was mounted well forward of the wing, the wind-tunnel-wall corrections at the location of the detector were negligibly small and were not incorporated in the results.

THEORETICAL ESTIMATES OF THE LOCAL FLOW

Method

A method of estimating upwash in the extended wing-chord plane for airplanes with swept wings is presented in reference 2. The method assumes that the total upwash angle is the sum of the individual upwash angles due to the presence of the wing, fuselage, and nacelle with the fuselage and nacelle acting in the upwash field of the wing. Lifting-surface theory of reference 3 is used to obtain the upwash due to the wing, while the upwash angles due to the nacelles and fuselage are obtained as in reference 4 from potential-flow equations, assuming the fuselage to be an infinite cylinder and the nacelles to be semi-infinite bodies of revolution. The method has been extended in reference 5 to cover regions above and below the wing-chord plane.

Application of the Method

The method of references 2 and 3 was used to obtain the upwash effects due to the wing on the wind-tunnel model. However, since the detector was rather near the nose of the fuselage, the semi-infinite body theory of reference 4 was used to obtain the upwash due to the influence of the fuselage rather than considering the fuselage to be an infinite cylinder.

As in reference 2, the local flow angle is equal to the geometric angle of attack plus the upwash due to the presence of the wing and fuselage; that is,

$$\alpha_I = \alpha_G + \epsilon_w + \epsilon_b$$

which can be written

$$\alpha_I = \alpha_G + \frac{d\epsilon_w}{dC_L} C_L + \frac{d\epsilon_b}{d\alpha} \left(\alpha_G + \frac{d\epsilon_w}{dC_L} C_L\right)$$

Then

$$\frac{\partial \alpha_I}{\partial \alpha_G} = 1 + \frac{d\epsilon_w}{dC_L}\frac{dC_L}{d\alpha_G} + \frac{d\epsilon_b}{d\alpha}\left(1 + \frac{d\epsilon_w}{dC_L}\frac{dC_L}{d\alpha_G}\right) \tag{1}$$

and

$$\frac{\partial \alpha_I}{\partial \delta_f} = \frac{d\epsilon_w}{dC_L}\frac{dC_L}{d\delta_f} + \frac{d\epsilon_b}{d\alpha}\frac{d\epsilon_w}{dC_L}\frac{dC_L}{d\delta_f} \tag{2}$$

Equation (1) is used to determine the slope of the curve of indicated angle of attack versus true angle of attack. The variation of upwash with lift coefficient, $d\epsilon_w/dC_L$, is obtained from the lifting-surface theory as applied in reference 2 (assuming an elliptic span load); the lift curve slope, $dC_L/d\alpha$, is obtained from experimental results (fig. 2); and the variation of upwash with angle of attack, $d\epsilon_b/d\alpha$, due to the presence of the fuselage, is obtained from potential flow equations for a semi-infinite body of revolution (ref. 4).

The effect of flap deflection on the local flow angle is obtained from equation (2). Again $d\epsilon_w/dC_L$ is obtained from lifting-surface theory (ref. 2), assuming an elliptic span load; the change in lift coefficient with flap deflection, $dC_L/d\delta_f$, is obtained from experimental results (cross plot of fig. 2); and $d\epsilon_b/d\alpha$ is obtained from potential-flow equations (ref. 4).

The method was applied to the F-86A-5 in essentially the same manner as for the wind-tunnel model except that the span load and lift-curve slope for the wing were obtained by use of reference 3.

RESULTS AND DISCUSSION

Triangular-Wing Model

The angle of attack indicated by the detector on the wind-tunnel model is shown as a function of the geometric angle of attack in figure 3. For comparison, the predicted variation is also shown for zero flap deflection. Although the agreement is not exact, it is considered adequate for preliminary calculations. The zero shift of about 0.2^{o} is attributed to the dissymmetry of the fuselage just aft of the location of the detector. (Since the shape of the fuselage at a moderate distance behind the detector has little effect on the calculated upwash, the fuselage was assumed to be a body of revolution as shown in fig. 1 for the purpose of calculation.) As for the discrepancy between the measured and predicted slopes of 0.10 (measured $d\alpha_T/d\alpha_G = 1.73$ and predicted $= 1.83$), most of the error is thought to be in the predicted value since the estimated accuracy of the measured slope is ± 0.02. The contribution of the wing upwash to the calculated slope was only 0.02, so it is apparent that the estimates of the upwash due to the fuselage must be charged with the major portion of the discrepancy. This indicates that the potential-flow equations as applied do not completely describe the flow around the fuselage just outside the boundary layer at the location of the detector.

To determine the effect of flap deflection, the increment of indicated angle of attack produced by flap deflection is shown in figure 4 as a function of flap deflection. Predicted results are included for comparison. The agreement between the measured and the predicted values is excellent. The effect of flap deflection is small at the location of the detector (1.2 semispans forward of the quarter-chord line) and could probably be neglected for most applications. If the detector were closer to the wing,[1] however, the change in upwash produced by the flap deflection would become large enough to be significant in fire-control use.

Flight Tests of F-86A-5

Figure 5 presents the comparison of the measured (ref. 1) and predicted slopes and intercepts of the indicated versus true angle-of-attack curves for the F-86A-5 airplane through the Mach number range.

---

[1] In the case of a swept wing the spanwise position is also a powerful factor in determining the amount of wing upwash, especially near the wing (see ref. 2).

Again the estimated slopes are higher than those actually measured.
It may be noted that the trends with increasing Mach number are in the
opposite direction. The theory also failed to predict the surprisingly
large variation of the intercept with Mach number. Since only 10 per-
cent of the calculated upwash is attributed to the wing (the detector
is 0.333 semispan forward of the quarter-chord line), it is apparent
that, again, the potential-flow equations used do not adequately
describe the flow at the location of the detectors which were outside
the boundary layer but near the surface of the fuselage.

In estimating the upwash angles, the fuselage was represented by
a semi-infinite body of revolution. It was assumed that there were no
effects of compressibility on the upwash due to the fuselage, and no
attempt was made to account for the air entering the inlet. The inlet-
flow and probable compressibility effects on the fuselage upwash may
account for a large portion of the discrepancy in slope shown in
figure 5. It is felt that the deviation of the actual fuselage from
the circular cross section used in the calculations combined with
compressibility effects is responsible for the poor correlation of the
measured intercept with that predicted.

CONCLUSIONS

Comparisons of predicted flow angles with those measured on the
forward portion of the fuselages of an aspect ratio 2 triangular-wing
wind-tunnel model and of an F-86A airplane in flight indicate the
following:

1. The accuracy of the predicted indicated angles of attack was
not sufficient to eliminate the necessity of a flight calibration of a
detector mounted on the fuselage. However, it did appear to be of
sufficient accuracy to be used for preliminary calculations in select-
ing the location of the detector and for the basic design of the
computer required to reduce the indicated to the true angle of attack.

2. The increase of upwash with flap deflection on the triangular-
wing wind-tunnel model was predicted accurately by the method described
herein.

3. The potential flow equations used to estimate the upwash due
to the presence of the fuselage did not completely describe the local
flow at the location of the detectors which were very close to the
fuselage but outside the boundary layer. The methods consistently
overestimated the indicated angle of attack.

4. At the location of the detector on the fuselage of the wind-tunnel model (1.2 semispans forward of the quarter-chord line), the change in upwash due to flap deflection was small and could be neglected for most applications.

Ames Aeronautical Laboratory
    National Advisory Committee for Aeronautics
        Moffett Field, Calif.

<div align="center">REFERENCES</div>

1. McFadden, Norman M., Rathert, George A., Jr., and Bray, Richard S.: Flight Calibration of Angle-of-Attack and Sideslip Detectors on the Fuselage of a 35° Swept-Wing Fighter Airplane. NACA RM A52A04, 1952.

2. Rogallo, Vernon L.: Effects of Wing Sweep on the Upwash at the Propeller Planes of Multiengine Airplanes. NACA TN 2795, 1952.

3. DeYoung, John, and Harper, Charles W.: Theoretical Symmetric Span Loading at Subsonic Speeds for Wings Having Arbitrary Plan Form. NACA Rep. 921, 1948.

4. Yaggy, Paul F.: A Method for Predicting the Upwash Angles Induced at the Propeller Plane of a Combination of Bodies With an Unswept Wing. NACA TN 2528, 1951.

5. Rogallo, Vernon L., McCloud, John L., III: Calculations of Upwash in the Region Above or Below the Wing-Chord Planes of Swept-Back Wing-Fuselage-Nacelle Combinations. NACA TN 2894, 1952.
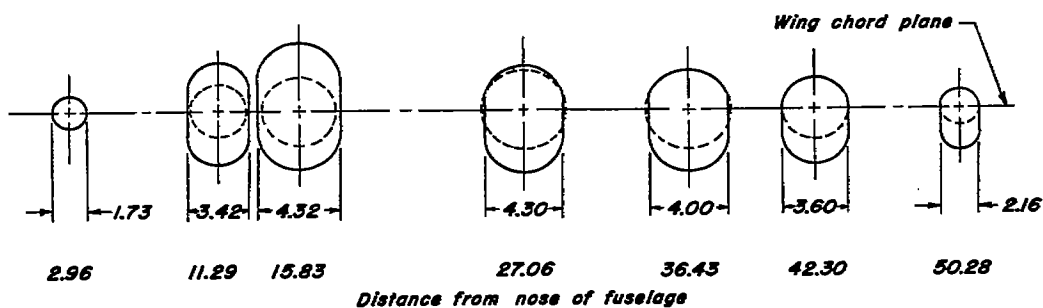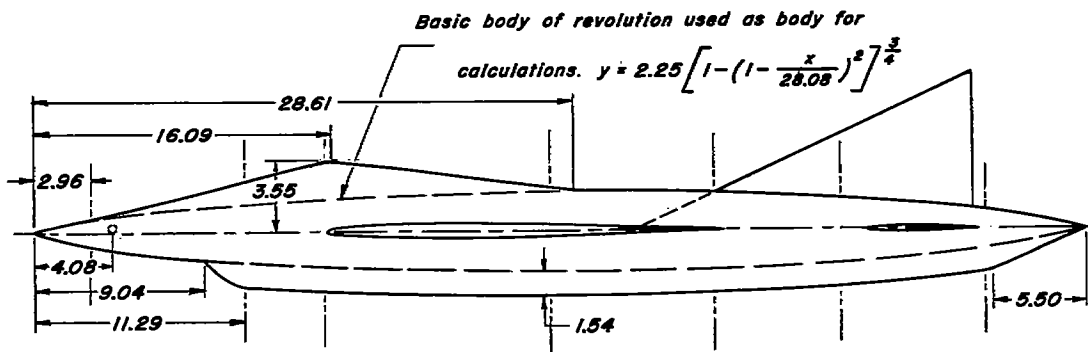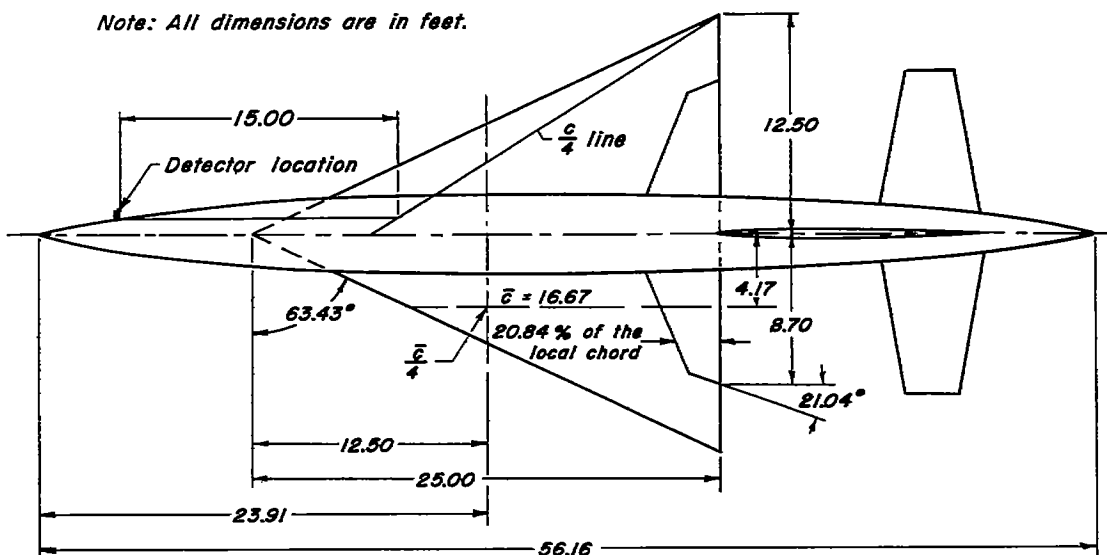
8

Note: All dimensions are in feet.

15.00

Detector location

$\frac{c}{4}$ line

12.50

63.43°

$\bar{c} = 16.67$

20.84 % of the local chord

$\frac{\bar{c}}{4}$

4.17

8.70

21.04°

12.50

25.00

23.91

56.16

Basic body of revolution used as body for calculations. $y = 2.25\left[1-\left(1-\frac{x}{28.08}\right)^2\right]^{\frac{3}{4}}$

28.61

16.09

2.96

3.55

4.08

9.04

11.29

1.54

5.50

Wing chord plane

1.73   3.42   4.32   4.30   4.00   3.60   2.16

2.96   11.29   15.83   27.06   36.43   42.30   50.28

Distance from nose of fuselage

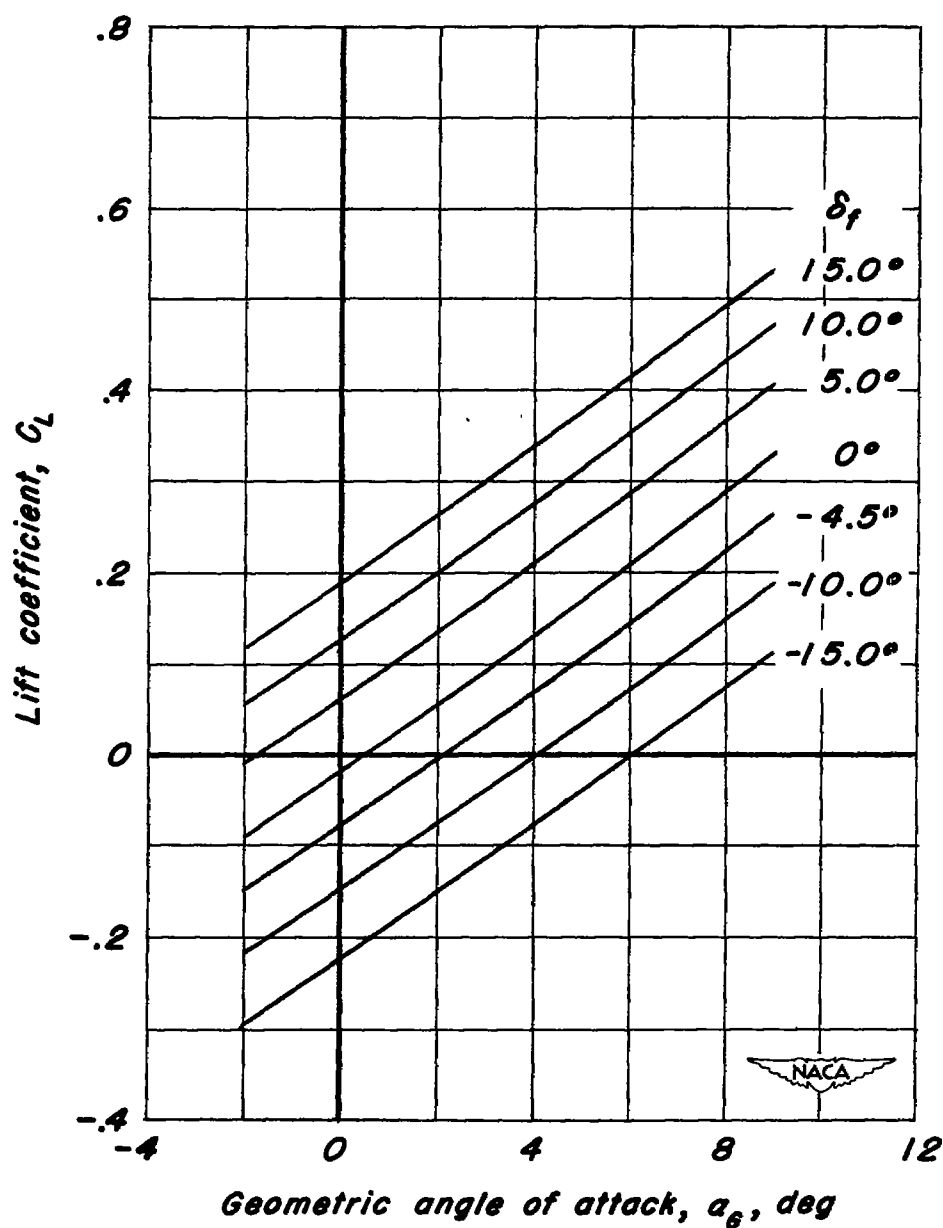*Figure 1.— Triangular-wing model used in 40-by 80-foot wind-tunnel tests.*

Figure 2.— Variation of lift coefficient with geometric angle of attack for various flap deflections. Triangular-wing model, 40-by 80-foot wind tunnel.
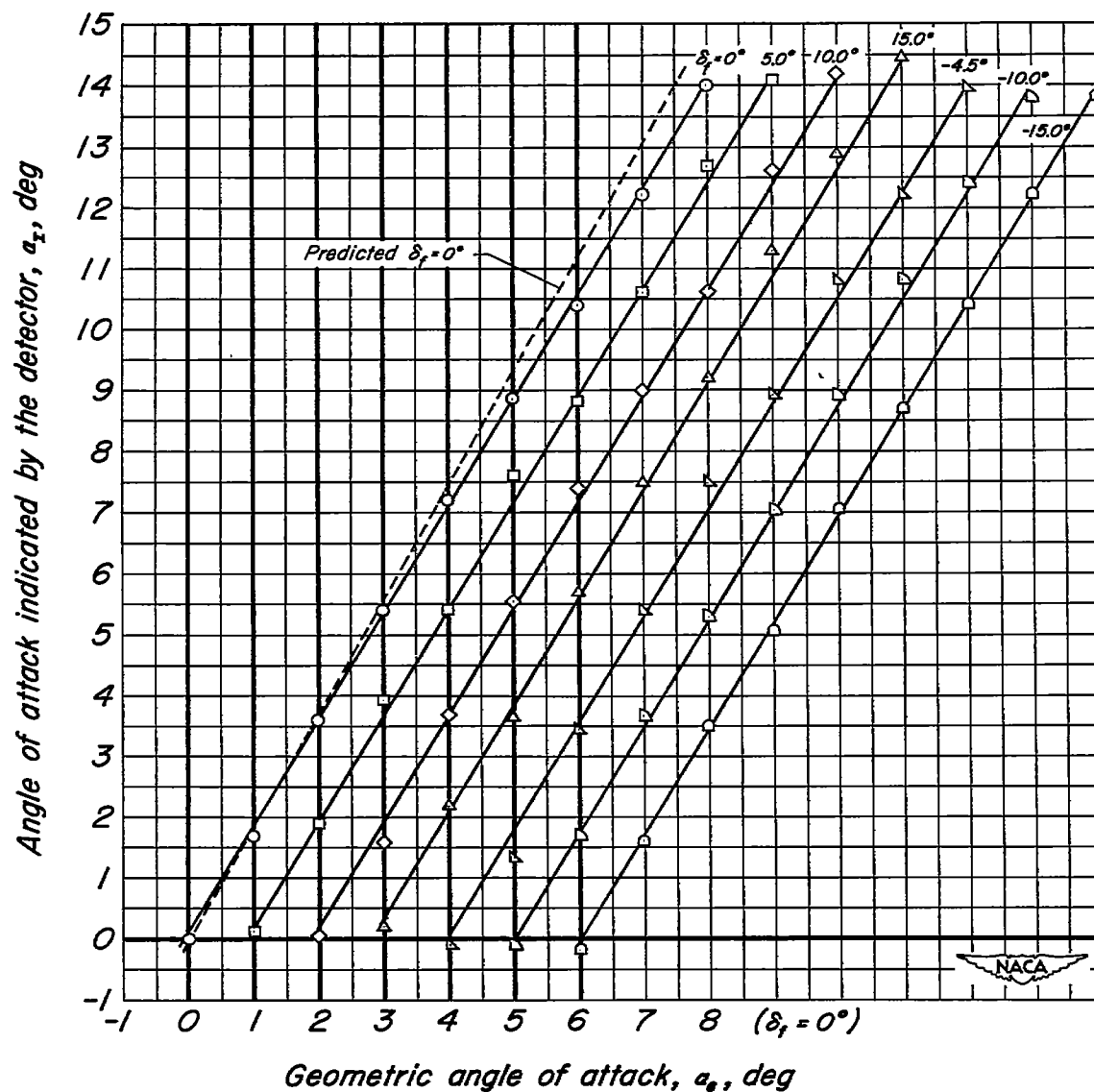
Figure 3.— Indicated angle of attack as a function of geometric angle of attack at various flap deflections. Triangular-wing model, 40-by 80-foot wind tunnel.
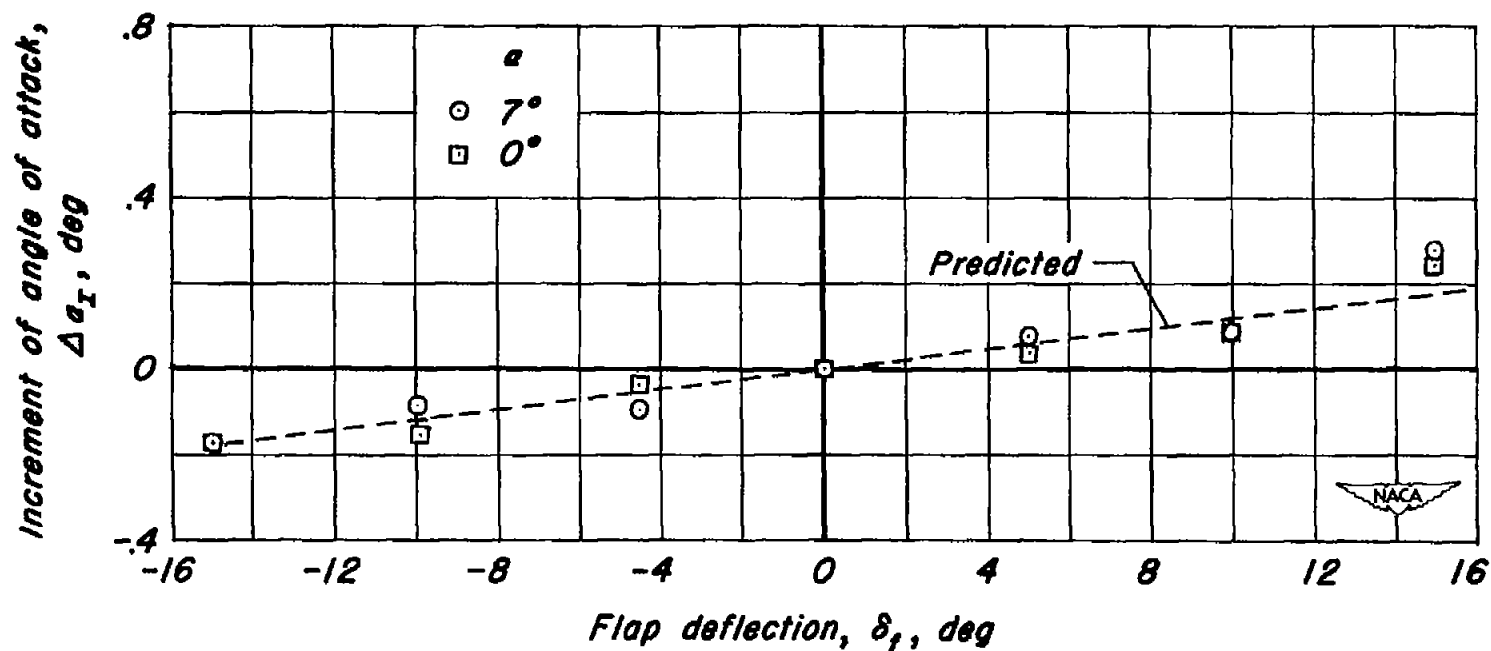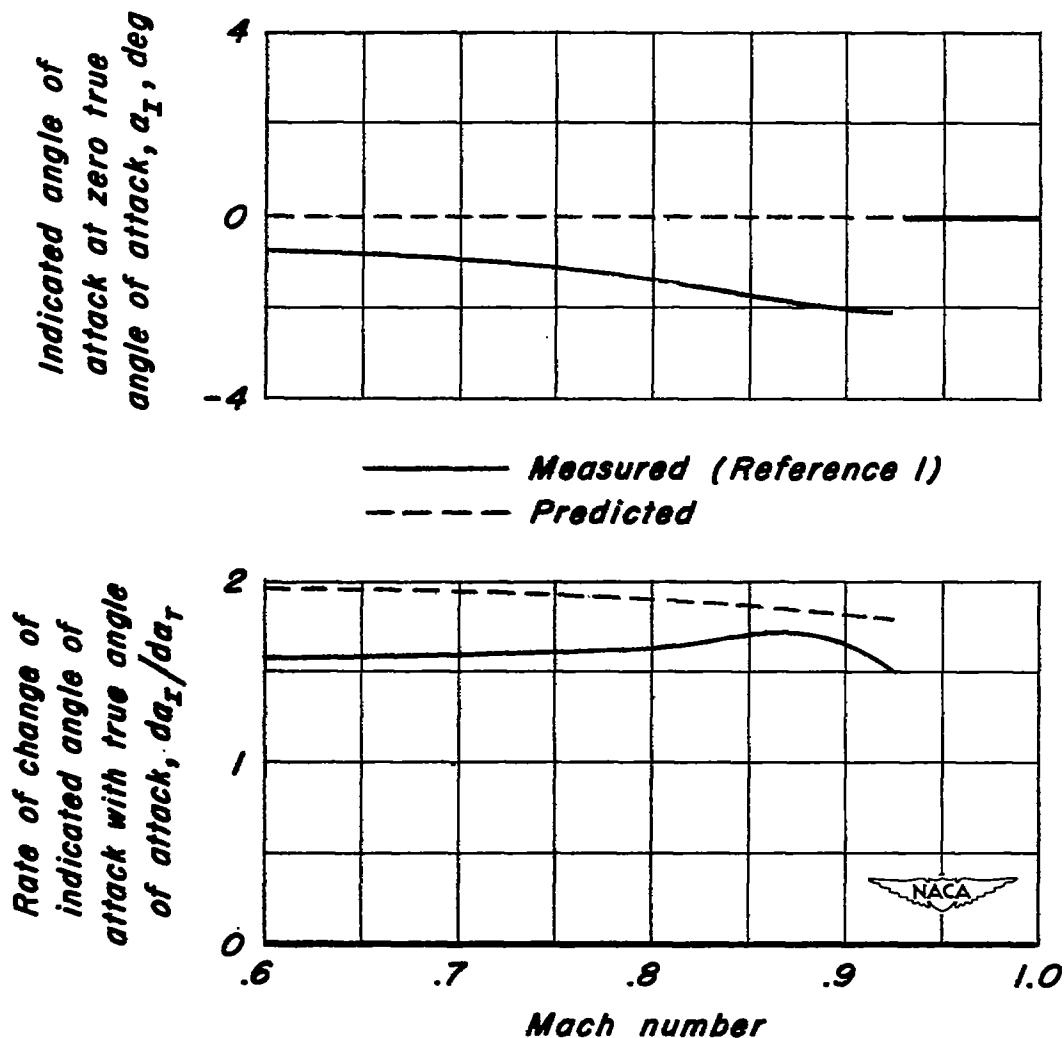
Figure 4.— The effect of flap deflection on the indicated angle of attack. Triangular-wing model, 40-by 80-foot wind tunnel.

Figure 5.— The variation with Mach number of the rate of change of indicated angle of attack with true angle of attack and the indicated angle of attack at zero true angle of attack for the F-86A-5 airplane.